In-Plane Magnetic Penetration Depth in Sr_2RuO_4: Muon-Spin Rotation and Relaxation Study

Rustem Khasanov,[1,*] Aline Ramires,[2] Vadim Grinenko,[3,4] Ilya Shipulin,[5] Naoki Kikugawa,[6] Dmitry A. Sokolov,[7] Jonas A. Krieger,[1] Thomas J. Hicken,[1] Yoshiteru Maeno,[8,9] Hubertus Luetkens,[1] and Zurab Guguchia[1]

[1]*Laboratory for Muon Spin Spectroscopy, Paul Scherrer Institut, CH-5232 Villigen PSI, Switzerland*
[2]*Laboratory for Theoretical and Computational Physics, Paul Scherrer Institut, CH-5232 Villigen PSI, Switzerland*
[3]*Tsung-Dao Lee Institute, Shanghai Jiao Tong University, Shanghai 201210, China*
[4]*School of Physics and Astronomy, Shanghai Jiao Tong University, Shanghai 200240, China*
[5]*Leibniz Institute for Solid State and Materials Research, 01069 Dresden, Germany*
[6]*National Institute for Materials Science, Tsukuba, Ibaraki 305-0003, Japan*
[7]*Max Planck Institute for Chemical Physics of Solids, Nöthnitzer Strasse 40, 01187 Dresden, Germany*
[8]*Department of Physics, Kyoto University, Kyoto 606-8502, Japan*
[9]*Toyota Riken - Kyoto University Research Center (TRiKUC), Kyoto 606-8501, Japan*

(Received 24 April 2023; revised 2 October 2023; accepted 3 October 2023; published 5 December 2023)

We report on measurements of the in-plane magnetic penetration depth (λ_{ab}) in single crystals of Sr_2RuO_4 down to $\simeq$0.015 K by means of muon-spin rotation-relaxation. The linear temperature dependence of λ_{ab}^{-2} for $T \lesssim 0.7$ K suggests the presence of nodes in the superconducting gap. This statement is further substantiated by observation of the Volovik effect, i.e., the reduction of λ_{ab}^{-2} as a function of the applied magnetic field. The experimental zero-field and zero-temperature value of $\lambda_{ab} = 124(3)$ nm agrees with $\lambda_{ab} \simeq 130$ nm, calculated based on results of electronic structure measurements reported in A. Tamai *et al.* [High-resolution photoemission on Sr_2RuO_4 reveals correlation-enhanced effective spin-orbit coupling and dominantly local self-energies, Phys. Rev. X **9**, 021048 (2019)]. Our analysis reveals that a simple nodal superconducting energy gap, described by the lowest possible harmonic of a gap function, does not capture the dependence of λ_{ab}^{-2} on T, so the higher angular harmonics of the energy gap function need to be introduced.

DOI: 10.1103/PhysRevLett.131.236001

The unconventional superconductivity in Sr_2RuO_4 attracts tremendous attention even after 30 years of its discovery [1]. The pure compound superconducts below $\simeq$1.5 K [2] and has a relatively simple, quasi-two-dimensional electronic structure with three nearly cylindrical Fermi surface sheets [3–8]. In addition, high quality crystals of Sr_2RuO_4 can be produced in large volumes [2,9] and the samples are clean [10–12], meaning that disorder is a less complicating factor in experiments as it is for most other unconventional superconductors.

One particular question to be answered is the symmetry of the superconducting order parameter. The linearity of the electronic specific heat capacity at low temperatures [13], the residual linear term of the in-plane thermal conductivity [14], the attenuation rate of ultrasound [15], and the field-oriented specific heat measurements [16] suggest the existence of nodes (or deep minima) in the superconducting gap. Recent thermal conductivity measurements for heat currents flowing parallel and perpendicular to the crystallographic c axis further indicate that these nodes or minima are oriented parallel to the c axis [17]. This finding was also supported by measurements of Bogoliubov quasiparticle interference, which allowed an identification of the position of the gap nodes in two Fermi surface sheets, and an estimate of the maximum value of the superconducting gap $\Delta^{max} \simeq 0.35$ meV [18].

Given the temperature dependence of the specific heat and thermal conductivity experiments [13,14,17], one expects a linear behavior of $\lambda^{-2}(T)$ at low temperatures. However, all experiments existing up to date report a power law dependence $\lambda^{-2}(T) \propto 1 - (T/T_c)^n$ with the exponent n ranging between 2 and 3 [19–22]. Such behavior was suggested to be consistent with the presence of nodes in the superconducting gap and ascribed to nonlocal electrodynamic effects leading to T^2 instead of linear behavior of $\lambda^{-2}(T)$ at low temperatures [19,23,24]. In this work, we report on measurements of the in-plane magnetic penetration depth λ_{ab} in high-quality single crystals of Sr_2RuO_4 ($T_c \simeq 1.4$ K, Ref. [25]) down to $T \simeq 15$ mK by means of muon-spin rotation and relaxation (μSR). The observed linear temperature dependence of λ_{ab}^{-2} for $T \lesssim T_c/2$ is consistent with the presence of nodes in the superconducting energy gap.

Single crystals of Sr_2RuO_4 were grown by the floating zone technique [9,29]. Several crystals were cleaved from rod n30 and mounted on the μSR sample holders [see Fig. 1(a) as an example for the transversal-field

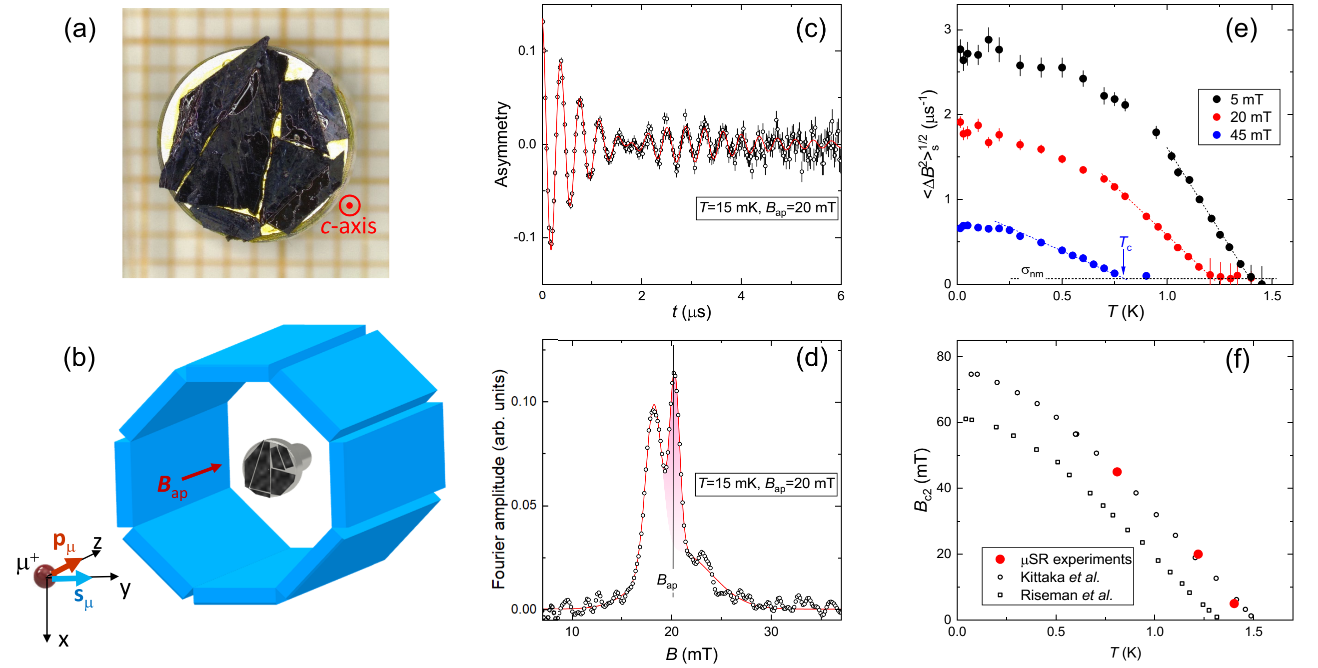

FIG. 1. (a) The c axis oriented Sr_2RuO_4 single crystals mounted on the HAL-9500 μSR sample holder. (b) Schematic view of the HAL-9500 experimental setup. Eight positron detectors are arranged in a ring surrounding the sample. The external magnetic field is applied along the muon momentum and parallel to the crystal's c axis ($\mathbf{B}_{ap} \| \mathbf{p}_\mu \| c$). The muon-spin $\mathbf{s}_\mu$ stays perpendicular to the applied magnetic field ($\mathbf{B}_{ap} \perp \mathbf{s}_\mu$). (c) Muon-time spectra collected at $T = 15$ mK and $B_{ap} = 20$ mT. (d) Fourier transform of the muon-time spectra shown in panel (c). The red area denotes the background contribution. The solid line in (c) and (d) are three-component fits [25]. (e) Temperature dependence of the square root of the second moment $\langle \Delta B^2 \rangle_s^{1/2}$ measured at $B_{ap} = 5$, 20, and 45 mT. The transition temperature T_c at $B = B_{ap}$ is defined by the intersection of the linearly extrapolated $\langle \Delta B^2 \rangle_s^{1/2}(T, B_{ap})$ close to T_c with the nuclear moment contribution, $\sigma_{nm} =$ const line. (f) Temperature dependence of the upper critical field $B_{c2}^{\|}$ obtained by Kittaka *et al.* [31] and Riseman *et al.* [32]. The red points are $B_{c2}^{\|}(T)$ values from this work.

setup]. The transverse-field μSR experiments were carried out at the πE3 beamline using the HAL-9500 spectrometer, the zero-field μSR data were collected at the πM3 beamline by using the newly built FLAME spectrometer (both at the Paul Scherrer Institute, Switzerland). A schematic representation of the experimental setup at the HAL-9500 instrument is shown in Fig. 1(b). The experimental data were analyzed using the MUSRFIT package [30].

Figure 1(c) shows the transverse-field (TF) μSR time spectra collected at $T = 15$ mK under the applied field $B_{ap} = 20$ mT. The corresponding Fourier transform, reflecting the internal field distribution [$P(B)$] in Sr_2RuO_4 in the superconducting state, is presented in Fig. 1(d). The sharp peak at $B = B_{ap}$ represents the residual background signal from muons missing the sample. The asymmetric $P(B)$ distributions possess the basic features expected for an ordered flux line lattice (FLL), namely: the cutoff at low fields, the peak shifted below B_{ap} and the tail towards the high field direction [33,34]. The μSR time spectra were fitted by using a three-component Gaussian expression with the first (the temperature and field independent) component corresponding to the background contribution $P_b(B)$ and another two components accounting for the asymmetric distribution $P_s(B)$ within the sample: $P(B) = P_b(B) + P_s(B)$ [25,34,35].

The temperature dependence of a square root of the second central moment of $P_s(B)$ measured at $B_{ap} = 5$, 20 and 45 mT [$\langle \Delta B^2 \rangle_s^{1/2}(T, B_{ap})$] is presented in Fig. 1(e). The nuclear dipole field contribution σ_{nm} is assumed to be temperature independent, and determined from data at $T > T_c$ [the horizontal solid line in Fig. 1(e)]. Note that a small relaxation caused by effects of time reversal symmetry breaking (see the Supplemental Material [25], and Refs. [20,36,37]) is 2 orders of magnitude smaller compared to the measured $\langle \Delta B^2 \rangle_s^{1/2}(T, B_{ap})$ values and does not influence the analysis of TF-μSR data. It is also important that the presence of the muon leads to only a limited and relatively localized perturbation to the local crystal structure of Sr_2RuO_4 [38], and, therefore, does not disturb the flux line structure.

The superconducting component $\langle \Delta B^2 \rangle_{sc}$ is obtained by subtracting σ_{nm} from the measured second moment: $\langle \Delta B^2 \rangle_{sc} = \langle \Delta B^2 \rangle_s - \sigma_{nm}^2$. Following Refs. [39,40], $\langle \Delta B^2 \rangle_{sc}$ is a function of the magnetic penetration depth

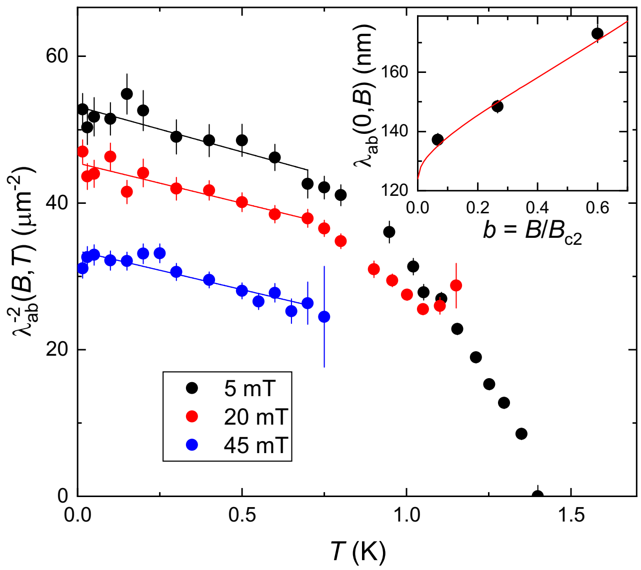

FIG. 2. λ_{ab}^{-2} vs T curves for Sr_2RuO_4 reconstructed from the measured $\langle \Delta B^2 \rangle_s^{1/2}(T)$'s presented in Fig. 1(e). The solid lines are linear fits for $T \lesssim 0.7$ K. The inset shows the dependence of the zero-temperature $\lambda_{ab}(0)$ on the reduced magnetic field $b = B/B_{c2}$.

λ and the reduced field $b = B/B_{c2}$:

$$\langle \Delta B^2 \rangle_{sc}^{1/2}\ [\mu s^{-1}] = A(1-b)[1 + 1.21 \times (1-\sqrt{b})^3]\lambda^{-2}\ [\mu m^{-2}]. \qquad (1)$$

Here B_{c2} is the upper critical field and A is a coefficient capturing the FLL symmetry. A is $\simeq$4.83 and 5.07 for the "hexagonal" and "square" FLL, respectively [40,41]. Note that, since in our experiments the magnetic field was applied along the crystallographic c axis [Figs. 1(a) and 1(b)], $\langle \Delta B^2 \rangle_{sc}^{1/2}$ is a function of the in-plane magnetic penetration depth λ_{ab} and B_{c2} in $\mathbf{B}_{ap} \| c$ orientation ($B_{c2}^{\|}$). Following Eq. (1), the temperature dependence of λ_{ab}^{-2} can be reconstructed from the measured $\langle \Delta B^2 \rangle_{sc}^{1/2}(T, B_{ap})$ if $B_{c2}^{\|}(T)$ is known. Figure 1(f) compares $B_{c2}^{\|}$ obtained from $\langle \Delta B^2 \rangle_s^{1/2}(T)$ curves measured at $B_{ap} = 5$, 20, and 45 mT with the literature data [31,32]. Good agreement is obtained with $B_{c2}^{\|}(T)$ from Kittaka *et al.* [31], which was further used in the $\lambda_{ab}^{-2}(T)$ reconstruction procedure. The FLL was assumed to be of a square symmetry, as reported in Refs. [21,32,42] for $B_{ap} \gtrsim 3.5$ mT.

Figure 2 shows λ_{ab}^{-2} vs T for $B_{ap} = 5$, 20, and 45 mT. From these data, the following three important points emerge: (i) Below $T \simeq 0.7$ K (i.e., for $T \lesssim T_c/2$) $\lambda_{ab}^{-2}(T)$ depends linearly on temperature. The linear fits result in similar values of $d\lambda_{ab}^{-2}/dT$ slopes, which is a clear indication of the presence of nodes in the superconducting gap; (ii) For $T \lesssim 0.7$ K the $\lambda_{ab}^{-2}(T)$ slopes are nearly parallel, suggesting $\lambda_{ab}^{-2}(T, B_{ap})$ values decrease with increasing B_{ap}. This is a manifestation of the so-called Volovik effect, which is caused by magnetic field-induced quasiparticle excitations around gap nodes [43,44]. (iii) The absolute value of the zero temperature and the zero field $\lambda_{ab}(0,0)$ could be obtained from its dependence on the reduced field b (see the inset in Fig. 2). According to Volovik [43], the density of excited states increases proportionally to $\sqrt{b}$, leading to [45,46]

$$\lambda(b)/\lambda(b=0) = (1 - K\sqrt{b})^{1/2}. \qquad (2)$$

Here K captures the strength of the Volovik effect. The solid line in the inset of Fig. 2 corresponds to the fit of Eq. (2) to the data with $K = 0.61(1)$ and $\lambda_{ab}(0,0) = 124(3)$ nm. To summarize, the results presented in Fig. 2 suggest the presence of nodes in the energy gap structure of Sr_2RuO_4, in agreement with the temperature dependencies of the thermal power and electronic specific heat, reported in Refs. [13,14,17].

The zero-temperature value of the in-plane penetration depth can also be calculated from the electronic band dispersion. For a quasi-two-dimensional superconductor, $\lambda^{-2}(0)$ can be written as [47]

$$\lambda_{ab}^{-2}(0) \equiv \sum_i \lambda_{ab,i}^{-2}(0) = \frac{e^2}{2\pi\varepsilon_0 c^2 h L_c} \sum_i \oint v_{F,i}(\mathbf{k}) dk. \qquad (3)$$

Here $\lambda_{ab,i}^{-2}(0)$ is the contribution of ith band to $\lambda_{ab}^{-2}(0)$, L_c is the c-axis lattice constant, $\mathbf{k}$ is a momentum vector, and v_F is the Fermi velocity. Integrations are made over the corresponding Fermi surface contours.

The Fermi surface of Sr_2RuO_4 consists of three nearly cylindrical sheets: α, β, and γ [the inset in Fig. 3(a)]. Precise ARPES measurements of the band structure and Fermi velocities were performed recently by Tamai *et al.* [7]. Using the band structure data from Ref. [7] the weight of each Fermi surface sheet to $\lambda_{ab}^{-2}(0)$ was found to be $\omega_\alpha \simeq 0.19$, $\omega_\beta \simeq 0.52$, and $\omega_\gamma \simeq 0.29$ [$\omega_i = \lambda_i^{-2}(0)/\lambda^{-2}(0)$]. The absolute value of λ_{ab} at $T = 0$ was estimated as $\lambda_{ab}(0) \simeq 130$ nm, in a good agreement with $\lambda_{ab}(0) = 124(3)$ nm obtained experimentally.

Figure 3(a) shows the temperature evolution of the superfluid density, $\rho_s(T) = \lambda_{ab}^{-2}(T)/\lambda_{ab}^{-2}(0)$. The data were reconstructed from $\lambda_{ab}^{-2}(T)$'s measured at $B_{ap} = 5$ and 20 mT (Fig. 2). In the clean limit, the temperature dependence of $\rho_s(T)$ can be theoretically estimated by [48]

$$\rho_s(T) = 1 + 2\int_{\Delta(T,\varphi)}^{\infty} \frac{\partial f(E,T)}{\partial E} D(E,T) dE, \qquad (4)$$

where $f(E,T) = [1 + \exp(E/k_B T)]^{-1}$ is the Fermi function, k_B is the Boltzmann constant, and $D(E,T)$ is the density of states (DOS) in the superconducting state

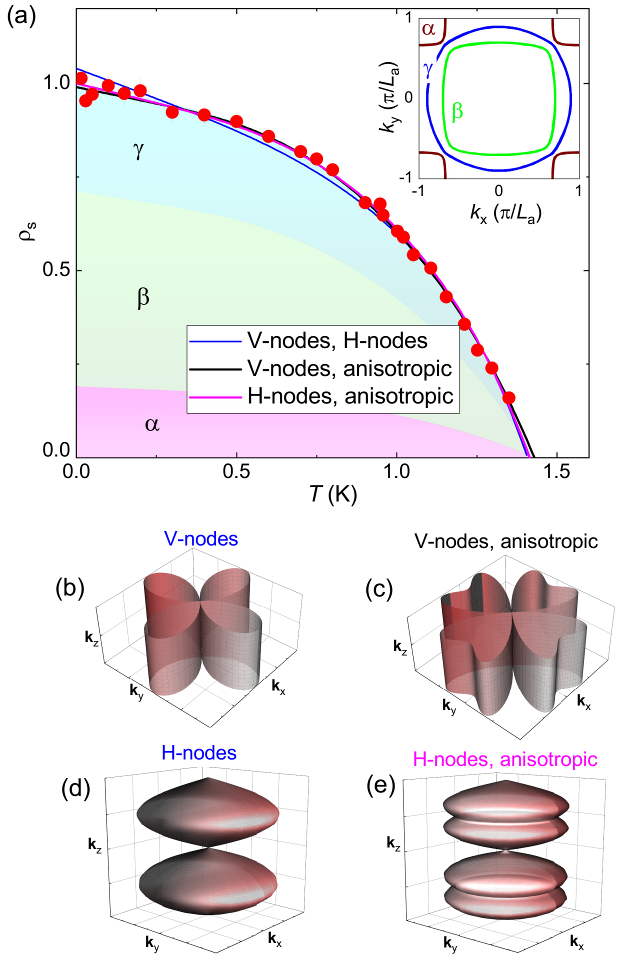

FIG. 3. (a) The temperature evolution of the superfluid density $\rho_s(T) = \lambda_{ab}^{-2}(T)/\lambda_{ab}^{-2}(0)$ of Sr_2RuO_4. The solid lines are fits using different vertical (V) and horizontal (H) nodal gap structures (see text for details). The colored areas represent contributions of the α, β, and γ Fermi surface sheets. The inset shows the first Brillouin zone of Sr_2RuO_4 with the α, β, and γ Fermi surface sheets. L_a is the a-axis lattice constant. (b),(c),(d), and (e) different nodal gap structures fitted to the experimental $\rho_s(T)$ data (see text for details).

normalized by its value in the normal state. For an s-wave superconductor $D(E,T) = E/\sqrt{E^2 - \Delta^2(T)}$, where $\Delta(T)$ is the magnitude of the superconducting gap at temperature T. A fully gapped superconductor has no DOS for $E < \Delta(T)$. As a consequence, the integral in Eq. (4) leads to an exponentially activated behavior for the superfluid density at the lowest temperatures $\rho_s(T) - \rho_s(0) \propto e^{-\Delta(0)/(k_B T)}$. Conversely, for a nodal superconductor, the DOS is obtained by an average over the Fermi surface, $\langle E/\sqrt{E^2 - \Delta^2(T,\mathbf{k})}\rangle_{FS}$, where $\Delta(T,\mathbf{k})$ is temperature and momentum dependent, with $\Delta(T,\hat{\mathbf{k}}_n) = 0$ along the nodal directions. The presence of nodes allows for quasiparticle excitations at arbitrarily low temperatures and fundamentally changes the result of the integral in Eq. (4). In particular, for line nodes one finds $\rho_s(T) - \rho_s(0) \propto T$ and for point nodes $\rho_s(T) - \rho_s(0) \propto T^2$, assuming a linearly vanishing gap at the nodes in both cases [49]. As the superfluid density is associated with a Fermi surface average, it is impossible to determine the position of nodes in momentum space solely from the information stemming from the $\rho_s(T)$. Nevertheless, the linear T dependence of $\rho_s(T)$ clearly suggests the presence of line nodes.

Fits of Eq. (4) to the experimental data were performed under the assumption of a quasi-2D (cylindrical) Fermi surface of Sr_2RuO_4 [50]. The superconducting gap function was assumed to depend on T and spherical angles φ and θ as $\Delta(T,\varphi,\theta) = \Delta g(\varphi,\theta)\tanh\{1.82[1.018(T_c/T - 1)]^{0.51}\}$ [Δ is the gap value at $T = 0$ and $g(\varphi,\theta)$ is the angular dependence of the gap] [51]. The presence of line nodes in the energy gap was accounted for by using following $g(\varphi,\theta)$ functions: $g_V(\varphi) = \cos(2\varphi)$ and $g_{V,an}(\varphi) = a_V\cos(2\varphi) + (1 - a_V)\cos(6\varphi)$ for vertical (V) nodes, and $g_H(\theta) = \sin(\theta)$ and $g_{H,an}(\theta) = a_H|\sin(\theta)| + (1 - a_H)|\sin(2\theta)|$ for horizontal (H) nodes, respectively. Here a_V and a_H are adjustable parameters. Note that $g_V(\varphi)$ corresponds to the "classical" gap of d-wave symmetry, while the "anisotropic" $g_{V,an}(\varphi)$ and $g_{H,an}(\varphi)$ functions contain terms corresponding to the next angular harmonic [52].

The results of the fits are shown by solid lines in Fig. 3(a) [53]. The corresponding $\Delta(\varphi,\theta)$ distributions are presented in panels (b),(c),(d), and (e). Note that the gap functions containing only the lowest possible harmonic [$\cos(2\varphi)$ or $\sin(\theta)$] do not agree with the experimental $\rho_s(T)$ data, while both anisotropic functional forms describe the data equally well. The maximum gap values and the adjustable parameters are $\Delta_V^{max} = \Delta_H^{max} = 0.388$ meV; $\Delta_{V,an}^{max} = 0.324$ meV, $a_V = 1.47$; and $\Delta_{H,an}^{max} = 0.348$ meV, $a_{H,an} = 0.55$ for the above described gap models. Note that the maximum gap values obtained from fits ($\Delta^{max} \simeq 0.32$–0.39 meV) stay in agreement with that measured directly by tunneling experiments ($\simeq$0.28–0.35 meV, Refs. [18,54]).

From the results presented above, the following points should be highlighted: (i) The temperature dependence of the superfluid density is equally well described by both vertical and horizontal line nodes [Fig. 3(a)]. (ii) The Volovik effect (the inset in Fig. 2) is active for a magnetic field component perpendicular to the Fermi velocity v_F. For $B_{ap}\|c$ and for a cylindrical Fermi surface, v_Fs point radially away from the center of the cylinder, so the Doppler effect shifts the nodes around the Fermi surface in the azimuthal direction. For vertical line nodes, the Doppler shift induces a finite quasiparticle DOS at the nodes and the Volovik effect is expected. For horizontal line nodes the Doppler shift takes the nodal structure into itself and does not introduce a finite density of states at the nodes. A more realistic treatment with three Fermi surfaces for Sr_2RuO_4 could lead to an observable Volovik effect even for horizontal line nodes [55,56]. The measurement of the penetration depth as a function of angles φ and θ may allow us to probe the gap anisotropy based on the angular dependence of the Volovik effect. (iii) Fits of Eq. (4) to $\rho_s(T)$ assume the same gap magnitude for all three (α, β, and γ) bands. If one allows the gap magnitudes to be different (i.e., $\Delta^{\max,\alpha} \neq \Delta^{\max,\beta} \neq \Delta^{\max,\gamma}$), and fit $\rho_s(T)$ following the weight determined by the electronic band structure, with $\rho_s(T) = \sum_i \omega_i \rho_{s,i}(T)$ ($i = \alpha$, β, or γ), no qualitative difference with the single-gap fits are found. The maximum gap values remain the same within ∼10%–20% accuracy.

Recently, multiple theoretical proposals focusing on even-parity superconducting states have emerged after the report on spin-singlet superconductivity by nuclear magnetic resonance experiments [57,58]. These proposals fall into three categories: (i) accidentally degenerate order parameters, such as $s \pm id$ [59] or $d \pm ig$ [60]; (ii) symmetry-protected two-component order parameters, such as chiral d wave; [61,62] (iii) single component order parameters with d-wave symmetry in the B_{1g} channel [63]. The $d + ig$ proposal in scenario (i) and the d-wave order parameter in scenario (iii) correspond to order parameters with symmetry protected vertical line nodes. These order parameters are completely compatible with our results, with the caveat that they develop with a nontrivial anisotropy captured by higher harmonic contributions to the gap structure. The $s + id$ proposal in scenario (i) does not have symmetry protected nodes, only gap minima. This could be compatible with our experiments as long as the gap minima are a small fraction of the gap maxima. The chiral order parameter proposed in scenario (ii) corresponds to an order parameter with symmetry protected horizontal line nodes, which would also be completely compatible with the observed temperature dependence of the penetration depth, as long as it is anisotropic in the sense discussed above. Concerning the Volovik effect, the order parameters that would most naturally capture this observation are the order parameters with vertical line nodes. Nevertheless, order parameters with multiple bands could also lead to such an effect even in the case of horizontal line nodes [55,56]. Interestingly, a recent proposal for a chiral d-wave order parameter suggests a combination of symmetry protected horizontal line nodes and vertical near nodes [61,64], which is also compatible with our observations. Our results provide strong evidence for gap nodes (or near nodes), but do not allow us to clearly rule out order parameters within the ones discussed above. In fact, even order parameters in the triplet sector, such as the ones discussed in Ref. [65] with vertical near nodes, could be compatible with our results. Note that more recent theoretical work based on spin-fluctuation mediated pairing [59], and calculations based on the random-phase approximation [66], find order parameters with strong azimuthal angular dependence also in the spin singlet sector. These theoretical results, obtained for various symmetry channels, are compatible with our conclusion that the superconducting gap has important contributions from high harmonics in a given symmetry channel.

To conclude, we report on measurements of the in-plane magnetic penetration depth in high-quality single crystals of Sr_2RuO_4 down to ultra-low temperature (≃0.015 K) by means of the muon-spin rotation and relaxation. The temperature evolution of λ_{ab}^{-2} represents pronounced linear behavior for temperatures $T \lesssim T_c/2$, in agreement with the presence of line nodes or deep minima in the superconducting gap. This picture is further confirmed by the reduction of $\lambda_{ab}^{-2}(0)$ with increasing applied field, a manifestation of the Volovik effect [43,44]. The zero-field and zero-temperature value of $\lambda_{ab} = 124(3)$ nm stays in agreement with $\lambda_{ab} \simeq 130$ nm calculated based on the electronic structure measured by means of ARPES [7]. The analysis of the temperature evolution of the superfluid density, reconstructed from the measured $\lambda_{ab}^{-2}(T, B_{ap})$ curves, reveals that the clean-limit behavior associated with the presence of a simple nodal superconducting gap described by the lowest possible angular harmonic does not account for the experimental data in the low temperature regime. To account for the low temperature behaviour, higher angular harmonics need to be introduced such that the low energy quasiparticle density of states is enhanced at low energies.

R. K. acknowledges helpful discussion with Clifford W. Hicks and support of Robert Scheuermann during the μSR experiments. Y. M., V. G., and N. K. are supported by JSPS Core-to-Core Program (No. JPJSCCA20170002). Y. M. is supported by JSPS KAKENHI (No. JP22H01168), and N. K. is supported by JSPS KAKENHI (No. JP18K04715, No. JP21H01033, and No. JP22K19093). A. R. acknowledges support from the Swiss National Science Foundation (SNSF) through an Ambizione Grant No. 186043. Z. G. acknowledges support from the Swiss National Science Foundation (SNSF) through SNSF Starting Grant (No. TMSGI2_211750). V. G. was supported by TDLI Start-up Grant.

*rustem.khasanov@psi.ch

[1] Y. Maeno, H. Hashimoto, K. Yoshida, S. Nishizaki, T. Fujita, J. G. Bednorz, and F. Lichtenberg, Superconductivity in a layered perovskite without copper, Nature (London) **372**, 532 (1994).

[2] Z. Q. Mao, Y. Maenoab, and H. Fukazawa, Crystal growth of Sr_2RuO_4, Mater. Res. Bull. **35**, 1813 (2000).

[3] A. P. Mackenzie, S. R. Julian, A. J. Diver, G. J. McMullan, M. P. Ray, G. G. Lonzarich, Y. Maeno, S. Nishizaki, and T. Fujita, Quantum oscillations in the layered perovskite superconductor Sr_2RuO_4, Phys. Rev. Lett. **76**, 3786 (1996).

[4] C. Bergemann, S. Julian, A. Mackenzie, S. NishiZaki, and Y. Maeno, Detailed topography of the fermi surface of Sr_2RuO_4, Phys. Rev. Lett. **84**, 2662 (2000).

[5] A. Damascelli, D. Lu, K. Shen, N. Armitage, F. Ronning, D. Feng, C. Kim, Z.-X. Shen, T. Kimura, Y. Tokura, Z. Mao, and Y. Maeno, Fermi surface, surface states, and surface reconstruction in Sr_2RuO_4, Phys. Rev. Lett. **85**, 5194 (2000).
[6] B. Burganov, C. Adamo, A. Mulder, M. Uchida, P. D. C. King, J. W. Harter, D. E. Shai, A. S. Gibbs, A. P. Mackenzie, R. Uecker, M. Bruetzam, M. R. Beasley, C. J. Fennie, D. G. Schlom, and K. M. Shen, Strain control of fermiology and many-body interactions in two-dimensional ruthenates, Phys. Rev. Lett. **116**, 197003 (2016).
[7] A. Tamai, M. Zingl, E. Rozbicki, E. Cappelli, S. Riccó, A. de la Torre, S. McKeown Walker, F. Y. Bruno, P. D. C. King, W. Meevasana, M. Shi, M. Radović, N. C. Plumb, A. S. Gibbs, A. P. Mackenzie, C. Berthod, H. U. R. Strand, M. Kim, A. Georges, and F. Baumberger, High-resolution photoemission on Sr_2RuO_4 reveals correlation-enhanced effective spin-orbit coupling and dominantly local self-energies, Phys. Rev. X **9**, 021048 (2019).
[8] Edgar Abarca Morales, Gesa-R. Siemann, Andela Zivanovic, Philip A. E. Murgatroyd, Igor Marković, Brendan Edwards, Chris A. Hooley, Dmitry A. Sokolov, Naoki Kikugawa, Cephise Cacho, Matthew D. Watson, Timur K. Kim, Clifford W. Hicks, Andrew P. Mackenzie, and Phil D. C. King, Hierarchy of Lifshitz transitions in the surface electronic structure of Sr_2RuO_4 under uniaxial compression, Phys. Rev. Lett. **130**, 096401 (2023).
[9] Jake S. Bobowski, Naoki Kikugawa, Takuto Miyoshi, Haruki Suwa, Han-shu Xu, Shingo Yonezawa, Dmitry A. Sokolov, Andrew P. Mackenzie, and Yoshiteru Maeno, Improved single-crystal growth of Sr_2RuO_4, Condensed Matter News **4**, 6 (2019).
[10] A. P. Mackenzie, S. R. Julian, A. J. Diver, G. G. Lonzarich, N. E. Hussey, Y. Maeno, S. Nishizaki, and T. Fujita, Calculation of thermodynamic and transport properties of Sr2RuO4 at low temperatures using known Fermi surface parameters, Physica (Amsterdam) **263C**, 510 (1996).
[11] Y. Maeno, K. Yoshida, H. Hashimoto, S. Nishizaki, S.-I. Ikeda, M. Nohara, T. Fujita, A. P. Mackenzie, N. E. Hussey, J. G. Bednorz, and F. Lichtenberg, Two-dimensional fermi liquid behavior of the superconductor Sr_2RuO_4, J. Phys. Soc. Jpn. **66**, 1405 (1997).
[12] C. Bergemann, A. P. Mackenzie, S. R. Julian, D. Forsythe, and E. Ohmichi, Quasi-two-dimensional fermi liquid properties of the unconventional superconductor Sr_2RuO_4, Adv. Phys. **52**, 639 (2003).
[13] S. Nishizaki, Y. Maeno, and Z. Mao, Changes in the superconducting state of Sr_2RuO_4 under magnetic fields probed by specific heat, J. Phys. Soc. Jpn. **69**, 572 (2000).
[14] M. Suzuki, M. A. Tanatar, N. Kikugawa, Z. Q. Mao, Y. Maeno, and T. Ishiguro, Universal heat transport in Sr_2RuO_4, Phys. Rev. Lett. **88**, 227004 (2002).
[15] C. Lupien, W. A. MacFarlane, Cyril Proust, Louis Taillefer, Z. Q. Mao, and Y. Maeno, Ultrasound attenuation in Sr_2RuO_4: An angle-resolved study of the superconducting gap function, Phys. Rev. Lett. **86**, 5986 (2001).
[16] K. Deguchi, Z. Q. Mao, H. Yaguchi, and Y. Maeno, Gap structure of the spin-triplet superconductor Sr_2RuO_4 determined from the field-orientation dependence of the specific heat, Phys. Rev. Lett. **92**, 047002 (2004).
[17] Elena Hassinger, Patrick Bourgeois-Hope, Haruka Taniguchi, Samuel Rene de Cotret, Gael Grissonnanche, M. Shahbaz Anwar, Yoshiteru Maeno, Nicolas Doiron-Leyraud, and Louis Taillefer, Vertical line nodes in the superconducting gap structure of Sr_2RuO_4, Phys. Rev. X **7**, 011032 (2017).
[18] Rahul Sharma, Stephen D. Edkins, Zhenyu Wang, Andrey Kostin, Chanchal Sow, Yoshiteru Maeno, Andrew P. Mackenzie, J. C. Séamus Davis, and Vidya Madhavan, Momentum resolved superconducting energy gaps of Sr_2RuO_4 from quasiparticle interference imaging, Proc. Natl. Acad. Sci. U.S.A. **117**, 5222 (2020).
[19] I. Bonalde, Brian D. Yanoff, M. B. Salamon, D. J. Van Harlingen, E. M. E. Chia, Z. Q. Mao, and Y. Maeno, Temperature dependence of the penetration depth in Sr_2RuO_4: Evidence for nodes in the gap function, Phys. Rev. Lett. **85**, 4775 (2000).
[20] G. Luke, Y. Fudamoto, K. Kojima, M. Larkin, B. Nachumi, Y. Uemura, J. Sonier, Y. Maeno, Z. Mao, Y. Mori, and D. Agterberg, Unconventional superconductivity in Sr_2RuO_4, Physica (Amsterdam) **289-290B**, 373 (2000).
[21] C. M. Aegerter, S. H. Lloyd, C. Ager, S. L. Lee, S. Romer, H. Keller, and E. M. Forgan, Evidence for a square vortex lattice in Sr_2 RuO_4 from muon-spin-rotation measurements, J. Phys. Condens. Matter **10**, 7445 (1998).
[22] P. J. Baker, R. J. Ormeno, C. E. Gough, Z. Q. Mao, S. Nishizaki, and Y. Maeno, Microwave surface impedance measurements of Sr_2RuO_4: The effect of impurities, Phys. Rev. B **80**, 115126 (2009).
[23] Hiroaki Kusunose and Manfred Sigrist, The penetration depth in Sr2RuO4: Evidence for orbital dependent superconductivity, Europhys. Lett. **60**, 281 (2002).
[24] Katsunori Kubo and Dai S. Hirashima, Magnetic penetration depth in quasi-two-dimensional superconductors with line nodes, J. Phys. Soc. Jpn. **69**, 3489 (2000).
[25] See Supplemental Material at http://link.aps.org/supplemental/10.1103/PhysRevLett.131.236001 for information on the specific heat measurements, the TF-μSR data analysis procedure, as well as the results of ZF-μSR experiments. The Supplemental Material includes Refs. [26–28].
[26] R. Khasanov, D. G. Eshchenko, D. Di Castro, A. Shengelaya, F. La Mattina, A. Maisuradze, C. Baines, H. Luetkens, J. Karpinski, S. M. Kazakov, and H. Keller, Magnetic penetration depth in $RbOs_2O_6$ studied by muon spin rotation, Phys. Rev. B **72**, 104504 (2005).
[27] R. S. Hayano, Y. J. Uemura, J. Imazato, N. Nishida, T. Yamazaki, and R. Kubo, Zero-and low-field spin relaxation studied by positive muons, Phys. Rev. B **20**, 850 (1979).
[28] V. Grinenko, S. Ghosh, R. Sarkar, J.-C. Orain, A. Nikitin, M. Elender, D. Das, Z. Guguchia, F. Brückner, M. E. Barber, J. Park, N. Kikugawa, D. A. Sokolov, J. C. Bobowski, T. Miyoshi, Y. Maeno, A. P. Mackenzie, H. Luetkens, C. W. Hicks, and H.-H. Klauss, Split superconducting and time-reversal symmetry-breaking transitions in Sr_2RuO_4 under stress, Nat. Phys. **17**, 748 (2021).
[29] N. Kikugawa, D. A. Sokolov, T. Nagasawa, and A. P. Mackenzie, Single-crystal growth of Sr_2RuO_4 by the floating-zone method using an infrared image furnace with improved halogen lamps, Crystals **11**, 392 (2021).

[30] A. Suter and B. M. Wojek, MUSRFIT: A free platform-independent framework for μSR data analysis, Phys. Procedia **30**, 69 (2012).

[31] S. Kittaka, T. Nakamura, Y. Aono, S. Yonezawa, K. Ishida, and Y. Maeno, Angular dependence of the upper critical field of Sr_2RuO_4, Phys. Rev. B **80**, 174514 (2009).

[32] T. M. Riseman, P. G. Kealey, E. M. Forgan, A. P. Mackenzie, L. M. Galvin, A. W. Tyler, S. L. Lee, C. Ager, D. McK. Paul, C. M. Aegerter, R. Cubitt, Z. Q. Mao, T. Akima, and Y. Maeno, Observation of a square flux-line lattice in the unconventional superconductor Sr_2RuO_4, Nature (London) **396**, 242 (1998).

[33] A. Maisuradze, R. Khasanov, A. Shengelaya, and H. Keller, Comparison of different methods for analyzing μSR line shapes in the vortex state of type-II superconductors, J. Phys. Condens. Matter **21**, 075701 (2009).

[34] Rustem Khasanov, Huaxue Zhou, Alex Amato, Zurab Guguchia, Elvezio Morenzoni, Xiaoli Dong, Guangming Zhang, and Zhongxian Zhao, Proximity-induced superconductivity within the insulating $(Li_{0.84}Fe_{0.16})$OH layers in $(Li_{0.84}Fe_{0.16})OHFe_{0.98}Se$, Phys. Rev. B **93**, 224512 (2016).

[35] R. Khasanov, A. Shengelaya, A. Maisuradze, F. La Mattina, A. Bussmann-Holder, H. Keller, and K. A. Müller, Experimental evidence for two gaps in the high-temperature $La_{1.83}Sr_{0.17}CuO_4$ superconductor, Phys. Rev. Lett. **98**, 057007 (2007).

[36] G. M. Luke, Y. Fudamoto, K. M. Kojima, M. I. Larkin, J. Merrin, B. Nachumi, Y. J. Uemura, Y. Maeno, Z. Q. Mao, Y. Mori, H. Nakamura, and M. Sigrist, Time-reversal symmetry-breaking superconductivity in Sr_2RuO_4, Nature (London) **394**, 558 (1998).

[37] Vadim Grinenko, Debarchan Das, Ritu Gupta, Bastian Zinkl, Naoki Kikugawa, Yoshiteru Maeno, Clifford W. Hicks, Hans-Henning Klauss, Manfred Sigrist, and Rustem Khasanov, Unsplit superconducting and time reversal symmetry breaking transitions in Sr_2RuO_4 under hydrostatic pressure and disorder, Nat. Commun. **12**, 3920 (2021).

[38] B. M. Huddart, I. J. Onuorah, M. M. Isah, P. Bonfà, S. J. Blundell, S. J. Clark, R. De Renzi, and T. Lancaster, Intrinsic nature of spontaneous magnetic fields in superconductors with time-reversal symmetry breaking, Phys. Rev. Lett. **127**, 237002 (2021).

[39] E. H. Brandt, Flux distribution and penetration depth measured by muon spin rotation in high-T_c superconductors, Phys. Rev. B **37**, 2349(R). (1988).

[40] E. H. Brandt, Properties of the ideal Ginzburg-Landau vortex lattice, Phys. Rev. B **68**, 054506 (2003).

[41] R. Khasanov, P. W. Klamut, A. Shengelaya, Z. Bukowski, I. M. Savić, C. Baines, and H. Keller, Muon-spin rotation measurements of the penetration depth of the Mo_3Sb_7 superconductor, Phys. Rev. B **78**, 014502 (2008).

[42] S. J. Ray, A. S. Gibbs, S. J. Bending, P. J. Curran, E. Babaev, C. Baines, A. P. Mackenzie, and S. L. Lee, Muon-spin rotation measurements of the vortex state in Sr_2RuO_4: Type-1.5 superconductivity, vortex clustering, and a crossover from a triangular to a square vortex lattice, Phys. Rev. B **89**, 094504 (2014).

[43] G. E. Volovik, Superconductivity with lines of gap nodes: Density of states in the vortex, JETP Lett. **58**, 469 (1993).

[44] N. B. Kopnin and G. E. Volovik, Singularity of the vortex density of states in d-wave superconductors, JETP Lett. **64**, 690 (1996).

[45] R. Kadono, Field-induced quasiparticle excitations in novel type II superconductors, J. Phys. Condens. Matter **16**, S4421 (2004).

[46] R. Khasanov, Takeshi Kondo, S. Strässle, D. O. G. Heron, A. Kaminski, H. Keller, S. L. Lee, and Tsunehiro Takeuchi, Zero-field superfluid density in a *d*-wave superconductor evaluated from muon-spin-rotation experiments in the vortex state, Phys. Rev. B **79**, 180507(R) (2009).

[47] D. V. Evtushinsky, D. S. Inosov, V. B. Zabolotnyy, M. S. Viazovska, R. Khasanov, A. Amato, H.-H. Klauss, H. Luetkens, Ch. Niedermayer, G. L. Sun, V. Hinkov, C. T. Lin, A. Varykhalov, A. Koitzsch, M. Knupfer, B. Büchner, A. A. Kordyuk, and S. V. Borisenko, Momentum-resolved superconducting gap in the bulk of $Ba_{1-x}K_xFe_2As_2$ from combined ARPES and μSR measurements, New J. Phys. **11**, 055069 (2009).

[48] M. Tinkham, *Introduction to Superconductivity* (Krieger Publishing, Malabar, Florida, 1975).

[49] F. Gross, B. S. Chandrasekhar, D. Einzel, K. Andres, P. J. Hirschfeld, H. R. Ott, J. Beuers, Z. Fisk, and J. L. Smith, Anomalous temperature dependence of the magnetic field penetration depth in superconducting UBe_{13}, Z. Phys. B **64**, 175 (1986).

[50] Andrew Peter Mackenzie and Yoshiteru Maeno, The superconductivity of Sr_2RuO_4 and the physics of spin-triplet pairing, Rev. Mod. Phys. **75**, 657 (2003).

[51] R. Khasanov, A. Shengelaya, A. Maisuradze, F. La Mattina, A. Bussmann-Holder, H. Keller, and K. A. Müller, Experimental evidence for two gaps in the high-temperature $La_{1.83}Sr_{0.17}CuO_4$ Superconductor, Phys. Rev. Lett. **98**, 057007 (2007).

[52] J. Mesot, M. R. Norman, H. Ding, M. Randeria, J. C. Campuzano, A. Paramekanti, H. M. Fretwell, A. Kaminski, T. Takeuchi, T. Yokoya, T. Sato, T. Takahashi, T. Mochiku, and K. Kadowaki, Superconducting gap anisotropy and quasiparticle interactions: A doping dependent photoemission study, Phys. Rev. Lett. **83**, 840 (1999).

[53] The fit of Eq. (4) to the data requires the value $\rho(0)$ to be model dependent and to deviate from unity. This is the case for $g_{\rm V}(\varphi) = \cos(2\varphi)$ and $g_{\rm H}(\theta) = \sin(\theta)$ gap models.

[54] H. Suderow, V. Crespo, I. Guillamon, S. Vieira, F. Servant, P. Lejay, J. P. Brison, and J. Flouquet, A nodeless superconducting gap in Sr_2RuO_4 from tunneling spectroscopy, New J. Phys. **11**, 093004 (2009).

[55] Yunkyu Bang, Volovik effect in the $\pm s$-wave state for the iron-based superconductors, Phys. Rev. Lett. **104**, 217001 (2010).

[56] Y. Wang, J. S. Kim, G. R. Stewart, P. J. Hirschfeld, S. Graser, S. Kasahara, T. Terashima, Y. Matsuda, T. Shibauchi, and I. Vekhter, Volovik effect in a highly anisotropic multiband superconductor: Experiment and theory, Phys. Rev. B **84**, 184524 (2011).

[57] A. Pustogow, Y. Luo, A. Chronister, Y. Su, D. Sokolov, F. Jerzembeck, A. Mackenzie, C. Hicks, N. Kikugawa, S. Raghu, E. Bauer, and S. Brown, Constraints on the superconducting order parameter in Sr_2RuO_4 from oxygen-17 nuclear magnetic resonance, Nature (London) **574**, 72 (2019).

[58] A. Chronister, A. Pustogow, N. Kikugawa, D. Sokolov, F. Jerzembeck, C. Hicks, A. Mackenzie, E. Bauer, and S. Brown, Evidence for even parity unconventional superconductivity in Sr_2RuO_4, Proc. Natl. Acad. Sci. U.S.A. **118** (2021).
[59] A. Rømer, D. Scherer, I. Eremin, P. Hirschfeld, and B. Andersen, Knight shift and leading superconducting instability from spin fluctuations in Sr_2RuO_4, Phys. Rev. Lett. **123**, 247001 (2019).
[60] S. Kivelson, A. Yuan, B. Ramshaw, and R. Thomale, A proposal for reconciling diverse experiments on the superconducting state in Sr_2RuO_4, npj Quantum Mater. **5**, 43 (2020).
[61] H. Suh, H. Menke, P. Brydon, C. Timm, A. Ramires, and D. Agterberg, Stabilizing even-parity chiral superconductivity in Sr_2RuO_4, Phys. Rev. Res. **2**, 032023(R) (2020).
[62] J. Clepkens, A. Lindquist, X. Liu, and H. Kee, Higher angular momentum pairings in interorbital shadowed-triplet superconductors: Application to Sr_2RuO_4, Phys. Rev. B **104**, 104512 (2021).
[63] R. Willa, M. Hecker, R. Fernandes, and J. Schmalian, Inhomogeneous time-reversal symmetry breaking in Sr_2RuO_4, Phys. Rev. B **104**, 024511 (2021).
[64] A. Ramires, Nodal gaps from local interactions in Sr_2RuO_4, J. Phys. Conf. Ser. **2164**, 012002 (2022).
[65] Thomas Scaffidi, Jesper C. Romers, and Steven H. Simon, Pairing symmetry and dominant band in Sr_2RuO_4, Phys. Rev. B **89**, 220510(R) (2014).
[66] X. Wang, Z. Wang, and C. Kallin, Higher angular momentum pairing states in Sr_2RuO_4 in the presence of longer-range interactions, Phys. Rev. B **106**, 134512 (2022).